COMPRESSION DESIGN OF HOLLOW COLD-FORMED HIGH STRENGTH STEEL SECTIONS

ANUP KC [1] and FATEMEH JAVIDAN [2]

[1,2]*Department of Science, Engineering and Technology, Federation University, Mt Helen, Victoria, Australia*

E-mail: anupkc@students.federation.edu.au [1]

E-mail: f.javidan@federation.edu.au [2]

Recent developments in technology and manufacturing of steel has led to a significant increase in the strength of steel material while keeping the weight constant. These developments have resulted in an increase in the application of high strength steel material in structural design and practice which has consequently led to a rising demand in updated design guidelines for structures consisting of these advanced materials. The present research covers the compression design of different grades of cold-formed circular hollow sections (CHS) including high strength steel (fy = 7700 MPa) and ultra-high strength steel material (fy =1250 MPa). Different section geometries are modelled using the numerical finite element software and are validated against available experimental tests. The validated result are then compared against available design guidelines in AS4100. The compressive performance is studied considering two types of slenderness ratios, namely the section slenderness and the member slenderness ratios. The results show that as the member slenderness and yield strength of the sections increase, the differences between the standard predictions becomes higher. Finally, these discrepancies are discussed and modifications are suggested.

Keywords: high strength steel tube, buckling, design guideline, compression.

1. Introduction

Various research has been conducted on High Strength Steel since the 1980s. The increasing developments in steel manufacturing has consequently led to a rising demand to apply these advances in structural engineering which requires updated design guidelines for structures consisting of advanced steel materials. In terms of compressive design, there are different factors which affect the performance of sections such as the section shape and the global and local buckling behaviour. Experiments done by Trigopula et.al. (2006) stated that the type of compressive force applied, ranging from instantaneous to long term also effects the compressive strength behaviour of the section. The paper concluded that Top Hat section were superior for the compression in short term impact but the square sections are more efficient in long run. Furthermore, the compression behaviour of the section was predicted according to the Australian standard i.e. AS4100:1998 and the results were analysed and compared against the experimental observations. As buckling, mainly local and distortional buckling affects the overall strength of high strength steel section, stress due to such types of buckling and their interaction plays vital role in the section design. Distortional buckling can be defined as the buckling characterized by rotation of flange at the junction of flange and web whereas in local buckling, plate like deformation occurs without translating the line of adjoining plates. In the experiment carried out by Hancock, G.J (1992), the buckling stress mainly due to distortional buckling was found to be

Proceedings of the 17th International Symposium on Tubular Structures.
Editors: X.D. Qian and Y.S. Choo

Published by Research Publishing, Singapore.
ISBN: 978-981-11-0745-0; doi:10.3850/978-981-11-0745-0_092-cd

smaller than that of yield stress for high strength steel samples. In mild steel samples from the experiments done by G.J Hancock (1994) in Hat and Channel section with yield stress of 200 to 480 MPa, yield stress was found to be smaller than that of distortional buckling stress. Hancock, G.J. et. al. (1994) gave some mathematical recommendations for the post buckling strength for the sections according to the yield stress. A research done by Ramussen and Hancock (1994) for columns with yield stress of 690 Mpa, the results were found to be conservative to Eurocode rather than other codes.

The current paper focuses on the compressive strength prediction of high strength steel circular tube sections according to the AS4100. Although the AS4100 standard provides design guidelines for steel material with yield strength up to 690 MPa, the current paper aims to investigate the compressive performance of steel columns with higher yield strength to propose possible modifications to the current guidelines. The yield strength of the steel materials considered for the tube sections are 770MPa and 1250MPa. Mild steel specimens have also been considered for comparison purposes. A finite element model simulating the buckling performance of high strength steel tubes is developed and validated against available experimental results. Non-linear analysis (Riks) has been used prior to which a buckling analysis has been performed introducing relevant imperfections to the model. The compressive strength of various geometries are then investigated and compared against the member capacities obtained from the AS4100 standard. According to the results, the increase in member slenderness and steel grade both result in higher discrepancies between the standard predictions, where some modifications are proposed accordingly.

1.1 *Geometrical specification*

Six different columns have been modelled initially to be compared against available experimental results. The labels, and geometrical specification and material types are introduced in Table 1. Cold-formed steel with high strength (HST) tube and ultra-high strength tube (UHST) sections are investigated. Mild tube (MT) has also been considered for comparison purposes. Specimens are in 1m or 2m lengths, which is specified at the end of the each specimen label. The tubes were tested for all three grades of steel and the results were analysed.

Table 1. Geometric specification

Specimen Label	Length (mm)	Outer diameter (mm)	Thickness (mm)	Steel types
MT-1	1000	76.1	3.2	Mild steel
HST-1	1000	76.1	3.2	High Strength Steel
UHST-1	1000	76.1	3.2	Ultra High strength steel
MT-2	2000	76.1	3.2	Mild steel
HST-2	2000	76.1	3.2	High strength steel
UHST-2	2000	76.1	3.2	Ultra high strength steel

2. Numerical Modelling and Verification

Analysis was done using the Finite Element software, ABAQUS. The boundary conditions were simulated according to the experimental test done by Javidan, F et. Al (2018) where the bottom end was fully fixed and the top end was fixed in all degrees of freedom except the displacement in the axial direction. Non-linear riks analysis has been performed. The numerical method consists of various steps upon which the correctness and adequacy of result is dependent. For the confirmation for mesh size for all the models, a mesh sensitivity analysis was performed

considering various mesh sizes (30, 20, 15, 12 and 8mm). From the mesh sensitivity analysis it was found that there were minor differences between the mesh sizes overall and the result started converging from 15 mm mesh size and lower. The mesh type used was an 8-noded quadrilateral element.

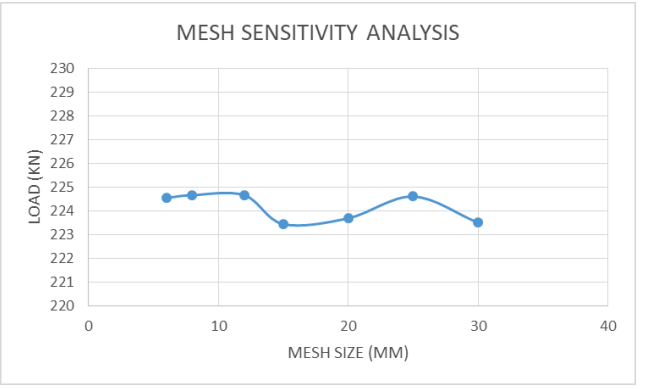

Figure 1. Mesh sensitivity analysis

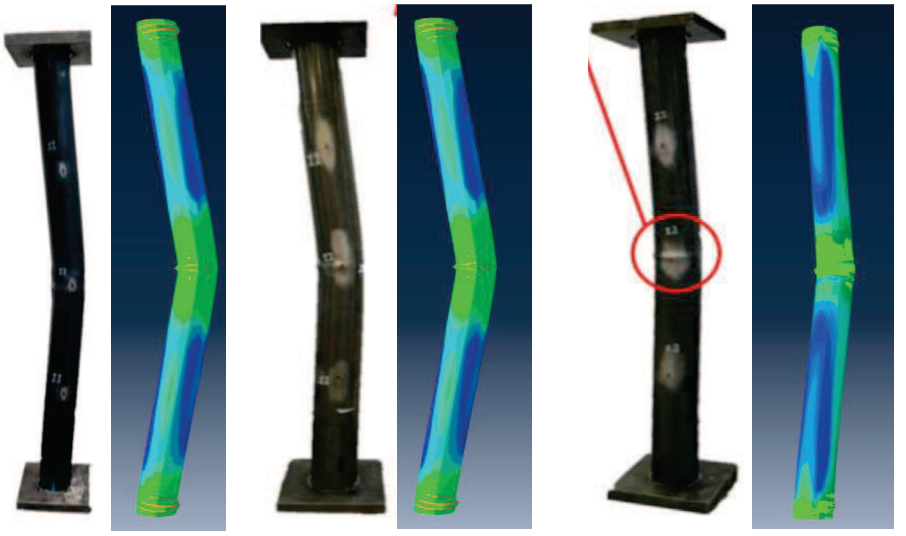

Figure 2. Comparison between failure mechanism in experimental and abaqus results for MT-1, HST-1 and UHST-1

The result from ABAQUS was compared with the experimental deformed shape and presented in Figures 2 and 3. The numerical model predicted the tube deformation very closely as it shows a reduction in the global buckling of tubes with higher yield strength values. The compressive strength of each specimen was also validated by comparing the load-displacement curves obtained from experiments. The model predicts the compressive capacity of specimens with an error of less than 5%. The slight discrepancy between the experimental and numerical results are understood to be due to the heat effects in the vicinity of the tube seem which is predicted to reduce the strength of material in the heat-affected region and has been ignored in this study.

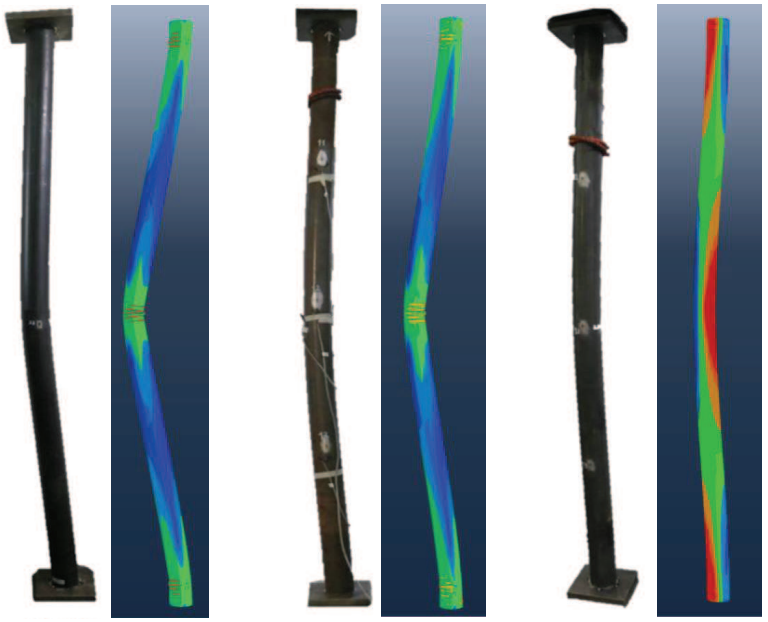

Figure 3. Comparison between failure mechanism in experimental and ABAQUS results for MT-2, HST-2 and UHST-2

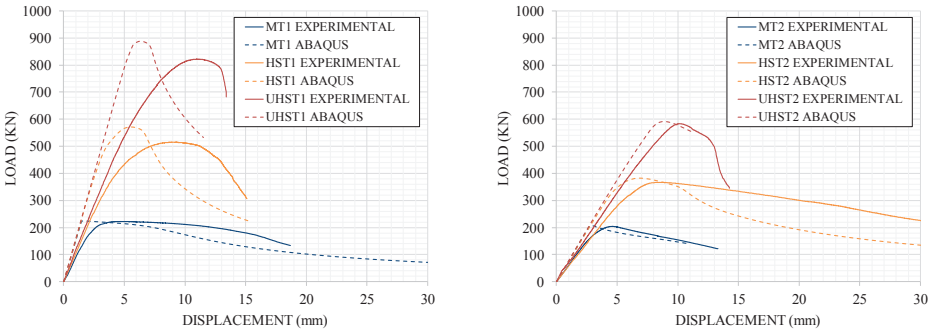

Figure 4. Graphical representation of model verification by comparing load-displacement curves of a) 1m and b) 2m samples

3. Results and Discussion

Further to the results obtained from the numerical model, the nominal member capacity in axial compression (N_C) of the tubes are also obtained from the AS4100 guidelines. The parameters for design are calculated as per the AS4100 and presented in Table 1. The design parameters are described as follows:

$$N_C = \alpha_C N_S \tag{1}$$

where N_S is defined as the compressive nominal section capacity, α_C is the compression member slenderness reduction factor. The modified compression member slenderness is also defined as follows:

$$\lambda_n = \frac{l_e}{r}\sqrt{k_f}\sqrt{\frac{f_y}{250}} \tag{2}$$

where r is the radius of gyration of the circular tube, k_f is form factor which is calculated from the ratio of gross area to the net area and is equal to 1. Due to the fixed boundary conditions at both ends, the member effective length factor (k_e) is 0.7. The effective length (Le) is ke * l (AS 4100:1998). The section slenderness limit is given as:

$$\lambda_s = \frac{d_o}{t} \times \frac{f_y}{250} \tag{3}$$

where, d_o is the outer diameter of the circular section and f_y is the yield stress of the steel material.

All section and slenderness values are calculated and presented in Table 2. Both the nominal compression section and member capacities are also obtained and shown. The actual compressive capacities obtained from the tests are also listed for further comparison. For better understanding of differences between the AS4100 code predictions and the experimental values, the results are compared visually in Figure 5.

Table 2. Design comparison of samples for 3.2mm diameter

Sample	effective length	f_y (MPa)	λ_s	α_c	N_S (kN)	λ_n	N_c (kN)	PEAK LOAD	Peak/Af_y
MT1	700	305	29.01	0.968	233.2	29.97	225.8	224.6	0.963
HST1	700	772	73.44	0.914	590.3	47.68	539.5	560.1	0.949
UHST1	700	1247	118.62	0.701	953.5	60.60	668.4	887.7	0.931
MT2	1400	305	29.01	0.862	233.2	59.94	201.0	208.1	0.892
HST2	1400	772	73.44	0.635	590.3	95.36	374.8	381.3	0.646
UHST2	1400	1247	118.62	0.456	953.5	121.20	434.8	591.1	0.620

Figure 5 shows the compressive capacity of steel tubes against the section slenderness. The graph also includes the comparison of the section slenderness limit to the limiting width and thickness ratio for circular hollow sections (CHS). The value is considered form table 5.2 AS 4100 in which the limit for circular hollow cold formed section is considered to be 50. The c/te for the limiting slenderness is hence 50. It can be seen that in slenderness limit value of 29.9 which corresponds to the MT section, the predicted compressive capacity of AS4100 matches to the values obtained from the tests. This is expected as the Mild steel is within the code's specified yield strength limits. For the HST with a slenderness limit of 59.9, the predictions are close to the

experimental observations as the yield strength of HST is only slightly above the specified yield limits. However, it is obvious from the graph that the UHST exhibits a higher compressive strength than what is predicted from the code. One important reason for this observation is the effect of yield strength in increasing the member slenderness which has resulted in a significant reduction in the predicted capacity. It can be concluded that there are modifications required for the nominal capacity of this steel material.

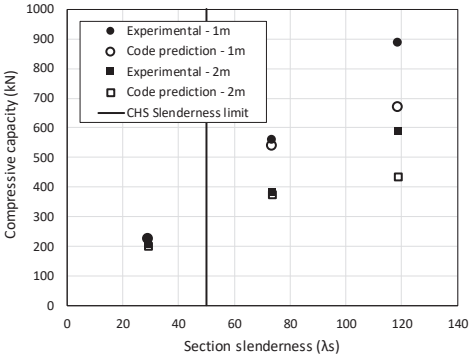

Figure 5. Comparison graph between Nc and Peak load

To further investigate the current code predictions in ultra-high strength tubes with various slenderness values, analysis has been conducted for a range of other thicknesses while keeping the diameter constant. These thicknesses are chosen according to the manufacturer's tables. The analysis is done for the peak load of HST and UHST which is compared to the values computed from AS4100, presented in Table 3 in detail.

Further to Table 3, a graphical representation is also shown in Figure 6. The vertical axis represents the ratio of peak load (compression capacity of tube section) to the nominal capacity predicted from the code (AS4100). These values are plotted versus the member slenderness values. The graph shows that with the increase in yield strength of sections, the ratio of the actual compressive strength to the predicted compressive strength increases. This ratio reaches higher values as the diameter to thickness ratio of the tube increases. Specifically, this ratio is equal to 1.66 for the UHST specimen with a thickness of 2.9mm and a length of 2 meters.

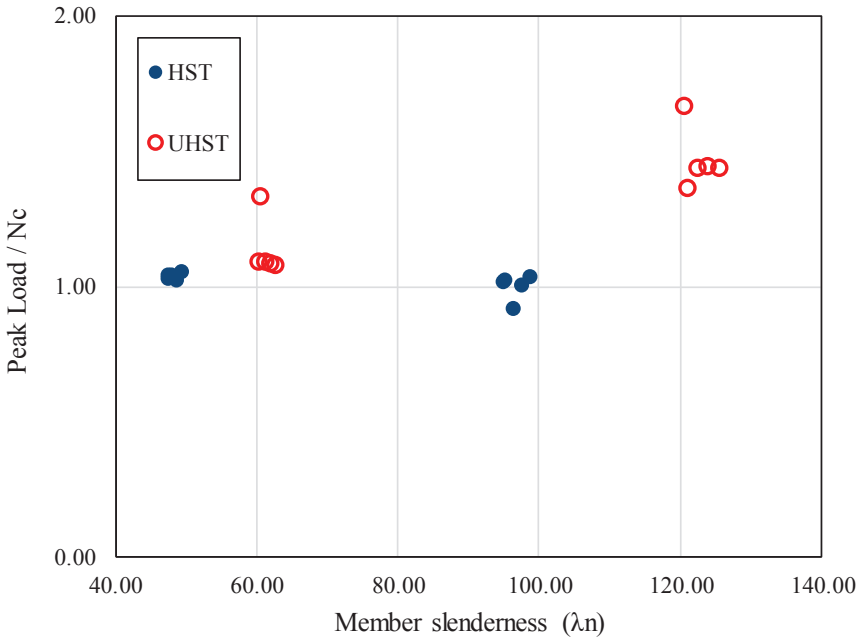

Figure 6. Slenderness limit comparisons

4. Conclusion

A numerical analysis has been completed for the hollow tubes with two different lengths and three types of steel material namely mild, high strength steel and ultra-high strength steel. The numerical model is developed and validated against available experimental results. Apart from the load-displacement curve and the predicated compressive capacity, the failure modes have also been compared and show matching results against the experiments. To check the extent of closeness of the available code prediction (AS4100) for steel grades higher than 690 MPa (which is specified as the upper limit in this code) further analysis has been conducted. As expected, the results showed a precise prediction of the compressive capacity of mild steel tubes. The high strength steel tube results also showed close comparison, whereas, the difference between those of ultra-high strength steel was significant. Further analysis was done for a wide range of thickness values to study the effect of slenderness on the variations between code prediction and the compression capacity. The code provisions were found to be underestimating the strength of UHST samples which increases with the rise in diameter to thickness ratios. The reason for this difference is due to the increase in member slenderness value with the increase in yield strength. Therefore, it can be concluded from the analysis result that the code provisions require a modification of up to 10% for HST section. This modification reaches 54-56% for UHST-2 specimens.

Table 3. Analysis result for various tube geometries

thickness	length	effective length	An	r	fy	αb	αc	NS(KN)			$\lambda_n = \frac{l_e}{r}\sqrt{k_f}\sqrt{\frac{f_y}{250}}$	$\frac{Peak\ load}{N_c}$	$\lambda_s = \frac{d_o}{t_e} * \frac{f_y}{250}$	$\frac{N_s}{Af_y}$	$\frac{Peak}{Af_y}$
								$N_s = k_f A_n f_y$	$N_c = \alpha_c N_s$	PEAK LOAD					
3.2	1000	700	764.65	25.80	772	-0.5	0.914	590.312	539.545	560.09	47.68	1.04	73.437	1	0.949
3.2	1000	700	764.65	25.80	1247	-0.5	0.701	953.522	668.419	887.66	60.60	1.33	118.621	1	0.931
3.2	2000	1400	764.65	25.80	772	-0.5	0.635	590.312	374.848	381.3	95.36	1.02	73.437	1	0.646
3.2	2000	1400	764.65	25.80	1247	-0.5	0.456	953.522	434.806	591.09	121.20	1.36	118.621	1	0.620
2.9	1000	700	692.97	25.90	772	-0.5	0.915	534.970	489.498	501.385	47.49	1.02	81.033	1	0.937
2.9	1000	700	692.97	25.90	1247	-0.5	0.864	864.129	746.608	812.46	60.36	1.09	130.892	1	0.940
2.9	2000	1400	692.97	25.90	772	-0.5	0.637	534.970	340.776	345.048	94.99	1.01	81.033	1	0.645
2.9	2000	1400	692.97	25.90	1247	-0.5	0.459	864.129	396.635	660.221	120.72	1.66	130.892	1	0.764
4	1000	700	955.82	25.53	772	-0.5	0.912	737.890	672.956	700.3	48.18	1.04	58.749	1	0.949
4	1000	700	955.82	25.53	1247	-0.5	0.868	1191.903	1034.571	1123	61.24	1.09	94.897	1	0.942
4	2000	1400	955.82	25.53	772	-0.5	0.642	737.890	473.725	433.978	96.36	0.92	58.749	1	0.588
4	2000	1400	955.82	25.53	1247	-0.5	0.449	1191.903	535.164	767.3	122.47	1.43	94.897	1	0.644
5	1000	700	1194.77	25.20	772	-0.5	0.91	922.362	839.350	857.963	48.81	1.02	46.999	1	0.930
5	1000	700	1194.77	25.20	1247	-0.5	0.872	1489.878	1299.174	1405.59	62.04	1.08	75.917	1	0.943
5	2000	1400	1194.77	25.20	772	-0.5	0.627	922.362	578.321	578.38	97.63	1.00	46.999	1	0.627
5	2000	1400	1194.77	25.20	1247	-0.5	0.439	1489.878	654.057	943.619	124.08	1.44	75.917	1	0.633
6	1000	700	1433.72	24.87	772	-0.5	0.907	1106.835	1003.899	1052.05	49.45	1.05	39.166	1	0.951
6	1000	700	1433.72	24.87	1247	-0.5	0.876	1787.854	1566.160	1684.38	62.85	1.08	63.264	1	0.942
6	2000	1400	1433.72	24.87	772	-0.5	0.613	1106.835	678.490	699.627	98.90	1.03	39.166	1	0.632
6	2000	1400	1433.72	24.87	1247	-0.5	0.43	1787.854	768.777	1100.82	125.70	1.43	63.264	1	0.616

References

Journal Papers

Ahmed, M., Liang, Q. Q., Patel, V. I., & Hadi, M. N. (2019). Numerical analysis of axially loaded circular high strength concrete-filled double steel tubular short columns. Thin-Walled Structures, 138, 105-116.

BAN*, H. Y., SHI, G., SHI, Y. J., & WANG, Y. Q. (2013). COLUMN BUCKLING TESTS OF 420 MPA HIGH STRENGTH STEEL SINGLE EQUAL ANGLES. International Journal of Structural Stability and Dynamics, 13(No. 2 (2013)), 1250069 (1250023 pages).

Ban, H. Y., Shi, G., Shi, Y. J., & Wang, Y. Q. (2011). Research progress on the mechanical property of high strength structural steels. Paper presented at the Advanced Materials Research.

Ban, H., & Shi, G. (2018). Overall buckling behaviour and design of high-strength steel welded section columns. Journal of Constructional Steel Research, 143, 180-195.

Ban, H., Shi, G., Shi, Y., & Wang, Y. (2012). Residual Stress Tests of High-Strength Steel Equal Angles. J. Struct. Eng.138(12), 1446-1454.

Chen, M.-T., & Young, B. (2019). Behavior of cold-formed steel elliptical hollow sections subjected to bending. Journal of Constructional Steel Research, 158, 317-330.

Chung, K. F., Ho, H. C., Wang, A. J., & Yu, W. K. (2016). Advances in Analysis and Design of Cold-Formed Steel Structures. Advances in Structural Engineering, vol. 11, 6, 615-632.

Hancock, G. J., Kwon, Y. B., & Bernard, S. E. (1994). Strength Design Curves for Thin-Walled Sections Undergoing Distortional Buckling. J. Construct. Steel Research 31 (1994), 169-186.

Huang, Z., Li, D., Uy, B., Thai, H.-T., & Hou, C. (2019). Local and post-local buckling of fabricated high-strength steel and composite columns. Journal of Constructional Steel Research, 154, 235-249.

Javidan, F., Heidarpour, A., Zhao, X.-L., & Minkkinen, J. (2016). Application of high strength and ultra-high strength steel tubes in long hybrid compressive members: Experimental and numerical investigation. Thin-Walled Structures, 102, 273-285.

Kwon, Y. B., & Hancock, G. J. (1992). Tests of cold-formed channels with local and distortional buckling. Journal of Structural Engineering, 118(7), 1786-1803.

Kwon, Y. B., Kim, B. S., & Hancock, G. J. (2009). Compression tests of high strength cold-formed steel channels with buckling interaction. Journal of Constructional Steel Research, 65(2), 278-289. doi:https://doi.org/10.1016/j.jcsr.2008.07.005

Li, H.-T., & Young, B. (2017). Tests of cold-formed high strength steel tubular sections undergoing web crippling. Engineering Structures, 141, 571-583.

Ma, J.-L., Chan, T.-M., & Young, B. (2015). Material properties and residual stresses of cold-formed high strength steel hollow sections. Journal of Constructional Steel Research, 109, 152-165. doi:https://doi.org/10.1016/j.jcsr.2015.02.006

Pham, C. H., & Hancock, G. J. (2010). Numerical simulation of high strength cold-formed purlins in combined bending and shear. Journal of Constructional Steel Research, 66(10), 1205-1217. doi:https://doi.org/10.1016/j.jcsr.2010.04.014

Rasmussen, K. J., & Hancock, G. J. (1992). Plate slenderness limits for high strength steel sections. Journal of Constructional Steel Research, 23(1-3), 73-96.

Rasmussen, K., & Hancock, G. (1995). Tests of high strength steel columns. Journal of Constructional Steel Research, 34(1), 27-52.

Shi, G., Zhou, W., & Lin, C. (2015). Experimental investigation on the local buckling behavior of 960 MPa high strength steel welded section stub columns. Advances in Structural Engineering, 18(3), 423-437.

Sun, Y., Liang, Y., & Zhao, O. (2019). Testing, numerical modelling and design of S690 high strength steel welded I-section stub columns. Journal of Constructional Steel Research, 159, 521-533.

Tarigopula, V., Langseth, M., Hopperstad, O. S., & Clausen, A. H. (2006). Axial crushing of thin-walled high-strength steel sections. International Journal of Impact Engineering, 32(5), 847-882.

Van Binh, D., Al-Mahaidi, R., & Zhao, X.-L. (2004). Finite element analysis (FEA) of fabricated square and triangular section stub columns utilizing very high strength steel tubes. Advances in Structural Engineering, 7(5), 447-460.

Young, B., & Lui, W. M. (2005). Behavior of Cold-Formed High Strength Stainless Steel Sections. J. Struct. Eng ,131(11), 1738-1745. doi:0.1061/_ASCE_0733-9445_2005_131:11_1738_

Yun, X., & Gardner, L. (2017). Stress-strain curves for hot-rolled steels. Journal of Constructional Steel Research 133 (2017), 36–46.

Standards

European Standard (1993), Eurocode 3 : Design of steel structures
Standards Australia (1998). Steel structures AS4100.
Standards Australia (2018), Cold formed steel structures AS 4600.